## PREPARATION AND PERFORMANCE OF $SrWO_4:RE^{3+}$ (RE = Eu, Sm, Pr) FLUORESCENT POWDERS FOR WHITE LEDs [**]

**Zhao Li[*], Ya-nan Wang, Kun-yao Wu, Yi-pu Xu, Jing Cao, Yong-feng Wang, Lu Deng**

*School of Materials Engineering of Xi'an Aeronautical University, Xi'an, China;*
*e-mail: pylizhao@163.com*

*The $SrWO_4:RE^{3+}$ (RE = Eu, Sm, Pr) fluorescent powders are synthesized using a high-temperature solid-state method. The phase structures and morphologies of the fluorescent powders are examined using X-ray diffraction and field-emission scanning electron microscopy, respectively. The results reveal that pure phase $SrWO_4$ can be prepared via calcination at 900 ℃ for 4 h and that doping with rare-earth ions has no effect on the crystal phase of the fluorescent powders; $SrWO_4$ powders doped with three rare earth ions all form spherical-like structures. The luminescence properties of the samples are evaluated using a fluorescence spectrometer, and the excitation and emission spectra of the $SrWO_4:RE^{3+}$ (RE = Eu, Sm, Pr) fluorescent powders are analyzed. The results indicate that $SrWO_4:Eu^{3+}$ fluorescent powder can be effectively excited by ultraviolet light at 395 nm and emit red light at 615 nm when a doping concentration of $Eu^{3+}$ is 7%; $Sm^{3+}$ and $Pr^{3+}$ doped $SrWO_4$ can emit red light at 650 and 687 nm when excited at 406 nm and 460 nm, respectively, with a doping concentration of 5% each. A W-LED device with $SrWO_4:Eu^{3+}$ pink fluorescent powder and a 395 nm UV chip is successfully assembled. The chromaticity coordinates of the device are (0.3055, 0.3532), exhibiting prominent white light. $SrWO_4:RE^{3+}$ (RE = Eu, Sm, Pr) fluorescent powders are expected to be red fluorescent powders for UV-excited white LEDs.*

***Keywords:*** *$SrWO_4$, rare earth ions, photoluminescence, W-LED device.*

## ПОЛУЧЕНИЕ И ПРИМЕНЕНИЕ ФЛУОРЕСЦЕНТНЫХ ПОРОШКОВ $SrWO_4:RE^{3+}$ (RE = Eu, Sm, Pr) ДЛЯ БЕЛЫХ СВЕТОДИОДОВ

**Z. Li[*], Y. Wang, K. Wu, Y. Xu, J. Cao, Y. Wang, L. Deng**

*УДК 535.37*

*Школа материаловедения Сианьского авиационного университета, Сиань, Китай;*
*e-mail: pylizhao@163.com*

*(Поступила 3 марта 2022)*

*Флуоресцентные порошки $SrWO_4:RE^{3+}$ (RE = Eu, Sm, Pr) синтезированы высокотемпературным твердотельным методом. Фазовая структура и морфология флуоресцентных порошков исследованы методами рентгеновской дифракции и автоэмиссионной сканирующей электронной микроскопии. Показано, что чистая фаза $SrWO_4$ может быть получена прокаливанием при 900°C в течение 4 ч и легирование редкоземельными ионами не влияет на кристаллическую фазу флуоресцентных порошков. Порошки $SrWO_4$, легированные тремя редкоземельными ионами, образуют сферические структуры. С помощью флуоресцентного спектрометра оценены люминесцентные свойства образцов, проанализированы спектры возбуждения и испускания флуоресцентных порошков $SrWO_4:RE^{3+}$ (RE = Eu, Sm, Pr). Показано, что флуоресцентный порошок $SrWO_4:Eu^{3+}$ может эффективно возбуждаться УФ-светом с $\lambda = 395$ нм и излучать красный свет с $\lambda = 615$ нм при концентрации $[Eu^{3+}] = 7$ %; $SrWO_4$, легированный $Sm^{3+}$ и $Pr^{3+}$, может излучать красный свет на $\lambda = 650$ и 687 нм при возбуждении на $\lambda = 406$ и 460 нм с концентрацией легирования 5 %. Изготовлено устройство W-LED с розовым флуоресцентным порошком $SrWO_4:Eu^{3+}$ и УФ-чипом 395 нм. Координаты цветности устройства (0.3055, 0.3532) демонстрируют ярко выраженный белый свет. Флуоресцентные*

[**] Full text is published in JAS V. 90, No. 3 (http://springer.com/journal/10812) and in electronic version of ZhPS V. 90, No. 3 (http://www.elibrary.ru/title_about.asp?id=7318; sales@elibrary.ru).

*порошки $SrWO_4:RE^{3+}$ (RE = Eu, Sm, Pr) могут найти применение в качестве компонентов красной флуоресценции для белых светодиодов с УФ-возбуждением.*

***Keywords:*** *$SrWO_4$, редкоземельные ионы, фотолюминесценция, устройство W-LED.*

**Introduction.** White LEDs are devices that emit white light at room temperature after their rare earth-doped fluorescent powder is excited by blue light chips or ultraviolet chips [1–4]. The realization of a photoluminescence phenomenon provides a new type of all-solid-state lighting source that is lauded as a fourth-generation lighting source due to its energy-savings, environmental protection, and green lighting advantages [5, 6]. The traditional realization method for white LED is mainly a combination of a blue LED chip and YAG:$Ce^{3+}$ yellow fluorescent powder. In this case, some of the blue light emitted by the blue LED is absorbed by YAG:$Ce^{3+}$ yellow fluorescent powder, which subsequently emits yellow light after excitation; the yellow light is mixed with some of the remaining blue light to produce white light [7, 8]. The main drawback of this combination is the low color rendering, which is caused by the lack of a red-light component in the YAG:$Ce^{3+}$ yellow fluorescent powder. At present, there is a significant paucity of red fluorescent powder that can be effectively excited by near UV light among fluorescent powder with high light conversion efficiency and excellent thermal stability.

Light with a wavelength of 395 and 465 nm can excite $Eu^{3+}$ ions from their ground state to the $^5L_6$ and $^5D_2$ energy levels, respectively, and these then relax to the $^5D_0$ energy level. Visible light of multiple wavelengths (595, 615, 655, and 705 nm) can be emitted (corresponding to $^5D_0 \rightarrow {}^7F_1$, $^7F_2$, $^7F_3$, and $^7F_4$ transitions, respectively). The emission of $Eu^{3+}$ is mainly centered at 615 nm. Peng Xiao [9] et al. designed a new high-temperature solid-phase approach to preparing $Sr_3LiSbO_6:Eu^{3+}$ red fluorescent powder. The influence of the $Eu^{3+}$ concentration on luminescence intensity was thoroughly investigated, and the XRD patterns, fluorescence spectra, fluorescence lifetimes, thermal stabilities, and chromaticity coordinates of samples were characterized and analyzed. The results indicate that the product can be excited by UV light and emits a stronger red light at 612 nm. Under excitation within 300–500 nm, $Sm^{3+}$ can undergo transitions from the ground state $^6H_{5/2}$ to the excited states $^4H_{7/2}$, $^4F_{9/2}$, $^4D_{5/2}$, $^4K_{11/2}$, $^4G_{9/2}$, and $^4I_{11/2}$, corresponding to wavelength ranges of 340–348, 353–365, 370–378, 399–407, 425–450, and 472–480 nm, respectively. The results reveal that $Sm^{3+}$ absorbs in the near-ultraviolet and blue light regions. Jiang Hongxi [10] et al. utilized the molten salt method to prepare $Sm^{3+}$ ion single-doped $NaIa(WO_4)_2:xSm^{3+}$ white fluorescent powder. Under ultraviolet light excitation, the blue-green light emitted via $WO_4^{2-}$ self-activation interacted with the green light emitted by $Sm^{3+}$, yellow light, orange light, and red light to generate white light. The fluorescent powder emits cool white light when excited at 250 nm, and warm white light when excited at 403 nm. $Pr^{3+}$ has a unique 4*f*, 5*d* electronic configuration, electronic transition structure, abundant electronic energy levels, and long-lived excited states due to its distinctive electronic layer structure. Li Zhao [11] et al. synthesized $SrMoO_4:Pr^{3+}$ red fluorescent powder using the hydrothermal method and studied the crystal structure, apparent morphology, and luminescence properties of fluorescent powder utilizing XRD, field-emission scanning electron microscopy (FSEM), and PL. The $SrMoO_4:Pr^{3+}$ fluorescent powder exhibits a spherical-like pure-phase structure with excitation peaks at 450, 473, and 485 nm and emission peaks at 606, 625, and 650 nm, respectively. The fluorescent powder emits a good red light at 650 nm and is compatible with blue LED chips. In many studies, rare earth metal-doped tungstate fluorescent powder has potential application prospects in the development of white light LEDs. However, research on rare earth-doped $SrWO_4$ fluorescent powder is still in its early stages. There are rare studies on the synthesis and luminescence properties of $Eu^{3+}$, $Sm^{3+}$, and $Pr^{3+}$-doped $SrWO_4$ fluorescent powders, especially in a high-temperature solid-phase environment. Therefore, it is necessary to investigate them in detail. In this paper, high-temperature solid-phase $SrWO_4$ fluorescent powders doped with the rare earth metal ions $Eu^{3+}$, $Sm^{3+}$, or $Pr^{3+}$, are synthesized, and the luminescence properties of the three fluorescent powders are thoroughly examined.

**Experimental.** Consider the preparation of $SrWO_4:Eu^{3+}$: stoichiometrically weighed amounts of $SrCO_3$, $WO_3$, and $Eu_2O_3$ (analytical grade) were placed in an agate mortar, followed by the addition of anhydrous ethanol, and thoroughly ground. The mixed system was placed in a corundum crucible and calcined at 900°C for 4 h. Finally, the product was ground to obtain $SrWO_4:Eu^{3+}$ fluorescent powder after cooling the crucible to room temperature in the furnace. The preparation methods for $SrWO_4:Sm^{3+}$ and $SrWO_4:Pr^{3+}$ fluorescent powders were identical as described above.

The XRD crystal structure of $SrWO_4:RE^{3+}$ (RE = Eu, Sm, or Pr) fluorescent powder was recorded on a Rigaku Ultima IV X-ray diffractometer (Rigaku Corporation, Japan) under the following conditions: Cu$K_\alpha$ target, 50 mA tube current, 40 kV tube voltage, 0.02° scanning step length, and 5–90° measurement range.

The surface morphologies were examined using a Zeiss Sigma 300 field-emission scanning electron microscope (Bruker, Germany). Before the test, the sample was ultrasonically dispersed in absolute ethanol for 10 min, and then air-dried, and gold-sputtered for 30 s. Excitation and emission spectra were obtained by a Hitachi F7000 fluorescence spectrophotometer (using a xenon lamp of 150 W, resolution of 1 nm, measuring range of excitation wavelengths of 200–500 nm, and emission wavelengths of 500–800 nm). The chromaticity coordinates and color-rendering index of the LED device were measured using a Hongpu HP9000 testing system. All of the tests were conducted at room temperature.

**Results and discussion.** *Structure analysis of $SrWO_4:RE^{3+}$ (Re = Eu, Sm, Pr).* XRD patterns of a $SrWO_4$ sample doped with the rare earth metal ions $Eu^{3+}$, $Sm^{3+}$, or $Pr^{3+}$ are shown in Fig. 1. These ions have a mole percentage of 0.07, 0.05, and 0.05, respectively, and the crystal structure of the sample remained unchanged after doping with rare earth metal ions. $SrWO_4$ has a scheelite structure, which is composed of a tetragonal crystal system with a space point group $I41/a(88)$ and unit cell parameters of $a$ = 5.4168 Å and $c$ = 11.951 Å. Furthermore, the positions of XRD peaks in the three samples are identical. The diffraction peaks of $SrWO_4:RE^{3+}$ (RE = Eu, Sm, Pr) fluorescent powders are the same as those of the standard card (JCPDS 08-0490), suggesting that they have the scheelite structure of the tungstate of alkaline earth metals.

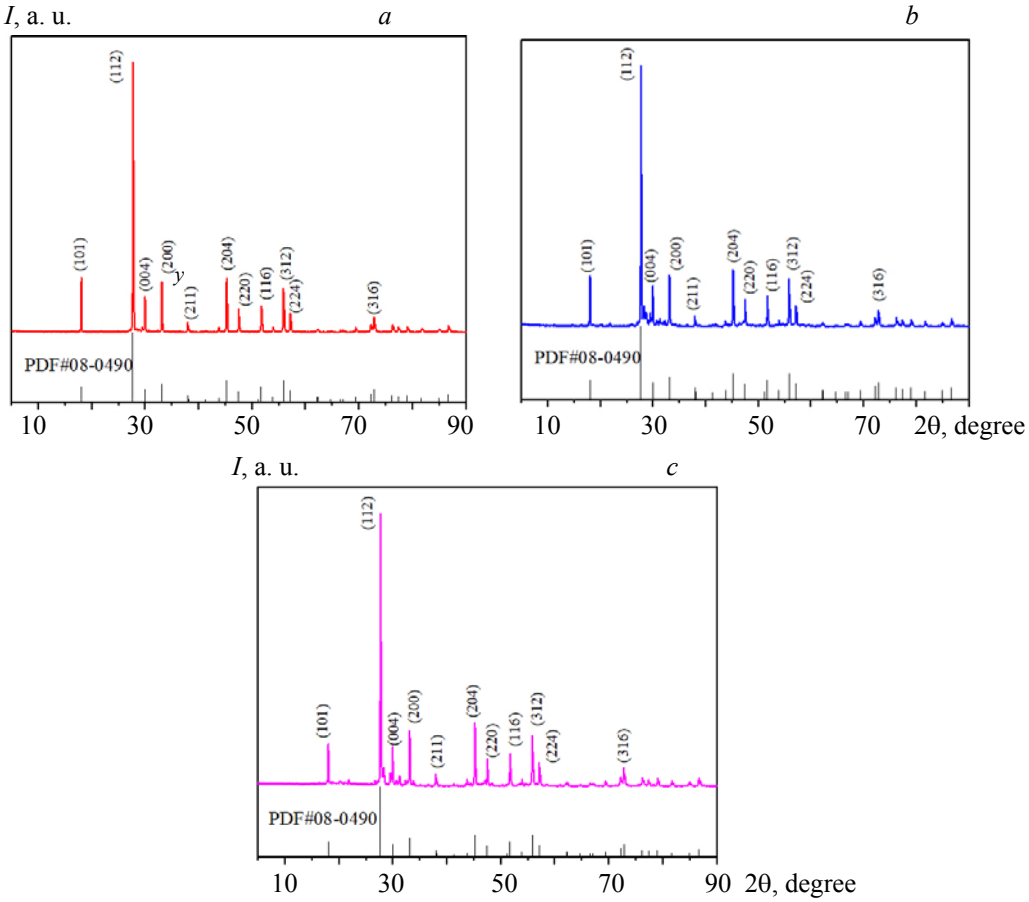


Fig. 1. XRD patterns of $SrWO_4:RE^{3+}$ (RE = Eu (a), Sm (b), and Pr (c)) phosphors.

Using the phase structure data of $SrWO_4:Eu^{3+}$ as an example, the Rietveld refinement is conducted to correct the crystal structure using the powder diffraction full-spectrum fitting method. The refined unit cell parameters are as follows: $a$ = 5.4156 Å, $b$ = 5.4156 Å, $c$ = 11.9530 Å, and $\alpha = \beta = \gamma = 90.000°$. Figure 2a illustrates that the reliability factors were $R_{wp}$ = 11.47% and $R_p$ = 7.25% after refinement; both values are less than 15%, indicating that the result of $SrWO_4:Eu^{3+}$ red fluorescent powder after XRD refinement is reliable. The modified structure of $SrWO_4$ is depicted in Fig. 2b. The $SrWO_4$ crystal belongs to the tetragonal crystal system, in which W and four O atoms form a tetrahedral $WO_4$, whereas Sr and six O atoms form an octahedral $SrO_6$; $WO_4$ and $SrO_6$ share one O atom.

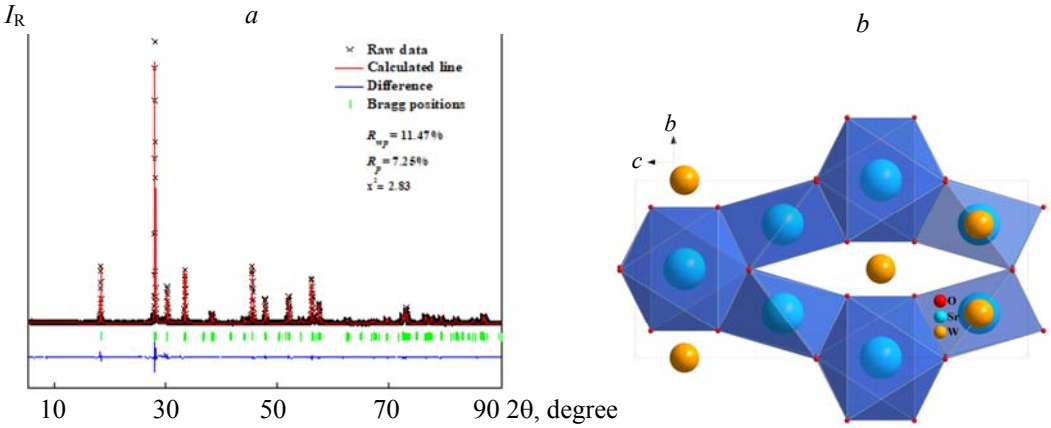


Fig. 2. Rietveld refinement (a) and the crystal structure of $SrWO_4$:7%$Eu^{3+}$ phosphors (b).

*Morphology analysis of $SrWO_4$:$RE^{3+}$ (RE = Eu, Sm, Pr) fluorescent powder.* Figure 3 depicts SEM micrographs and mapping spectra of $SrWO_4$ samples doped with the rare earth metal ions $Eu^{3+}$, $Sm^{3+}$, or $Pr^{3+}$. The spherical-like morphology of $SrWO_4$ powder that was synthesized using the high-temperature solid-phase method and doped with $Eu^{3+}$, $Sm^{3+}$, or $Pr^{3+}$ has a powder particle size of about 1 μm. The morphology and particle size of $SrWO_4$-type fluorescent powder are unaffected by doping with different rare-earth ions.

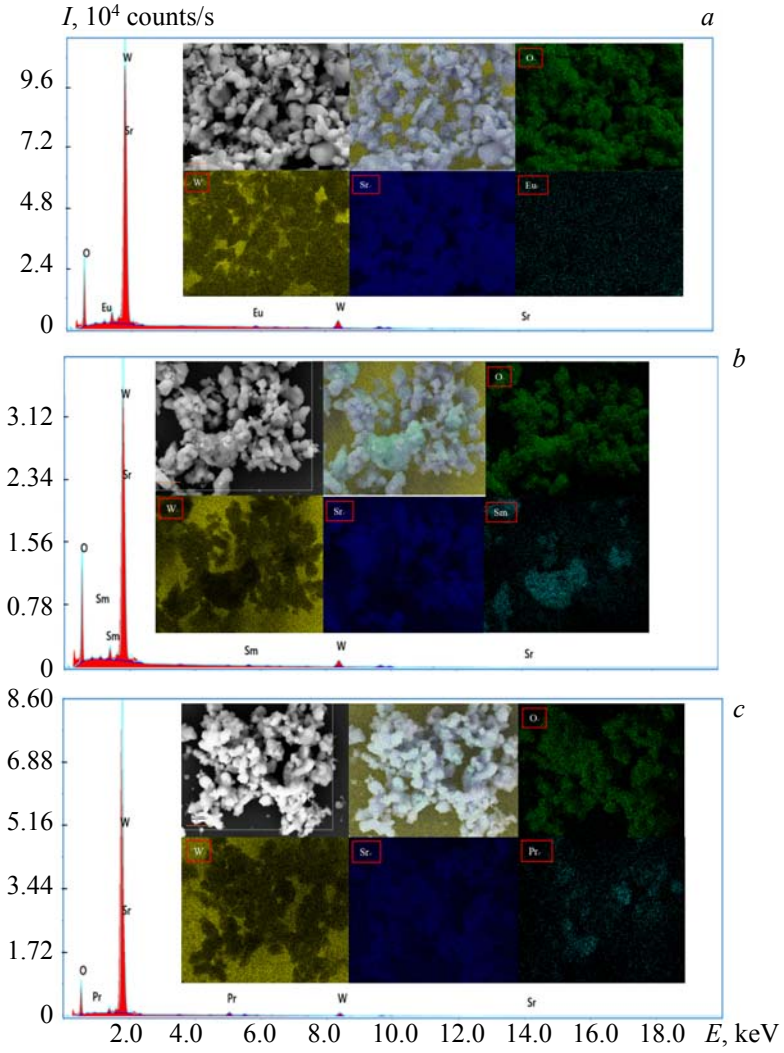


Fig. 3. SEM and mapping images of $SrWO_4$:$RE^{3+}$ (RE = Eu (a), Sm (b), and Pr(c)) phosphors.

The particle size of a fluorescent powder greatly influences its luminescence. Specifically, the fluorescent powder can be unevenly coated if the particle size is too large, whereas the absorption of UV light can be reduced if the particle size is too small; this increases ultraviolet radiation and reduces luminescence efficiency [12]. After integrated consideration, a particle size of 1–3 μm seems appropriate for the encapsulation of fluorescent powder and has good luminescence properties. The morphology and particle size of $SrWO_4:RE^{3+}$ (Re = Eu, Sm, Pr) fluorescent powder can be effectively controlled by using a simple high-temperature solid-phase synthesis. The mapping scan of the prepared $SrWO_4:Re^{3+}$ (Re = Eu, Sm, Pr) fluorescent powder reveals that the product is composed of four elements (O, W, Sr, and $Re^{3+}$) with no other elements, demonstrating that the rare earth ions, which are the luminescent sources, have been successfully doped into the target product. When the phase structure of the product is investigated, it is evident that the $SrWO_4:RE^{3+}$ (Re = Eu, Sm, Pr) fluorescent powders prepared in this study are pure-phase powders.

*Luminescence characteristics of $SrWO_4:RE^{3+}$ (RE = Eu, Sm, Pr) fluorescent powder.* Figure 4 depicts the excitation and emission spectra of the rare earth metal $Eu^{3+}$-doped $SrWO_4:Eu^{3+}$ fluorescent powder. Figure 4a illustrates the excitation spectrum of $SrWO_4:Eu^{3+}$ fluorescent powder at 616 nm. The strongest excitation peaks of the sample's excitation spectrum are located around 395 nm ($^7F_0 \rightarrow {}^5L_6$) and 465 nm ($^7F_0 \rightarrow {}^5D_2$). The 395 nm UV light and 465 nm blue light can effectively excite the $Eu^{3+}$-doped $SrWO_4$ fluorescent powder. Figure 4b displays the emission spectrum of the synthesized $SrWO_4:Eu^{3+}$ fluorescent powder at 395 nm. The emission peaks of the $SrWO_4:Eu^{3+}$ fluorescent powder 540 nm ($^5D_1 \rightarrow {}^7F_2$ or $^5D_2 \rightarrow {}^7F_4$), 591 nm ($^5D_0 \rightarrow {}^7F_1$), and 616 nm ($^5D_0 \rightarrow {}^7F_2$), as shown in Fig. 4b; the peak at 616 nm is the dominant emission peak. The reason for this is that when rare-earth ions are at lattice sites with inversion centers, only magnetic dipole transitions are allowed; however, when the ions are at lattice sites without an inversion center, rare-earth ion-forced electric dipole transitions are allowed [13, 14]. The intensity of the electric dipole transition $^5D_0 \rightarrow {}^7F_2$ in the emission spectrum of $SrWO_4:Eu^{3+}$ fluorescent powder is greater than that of the magnetic dipole transition $^5D_0 \rightarrow {}^7F_1$, indicating that $Eu^{3+}$ ions are at lattice sites without a symmetry center.

Figures 4c,d show the excitation and emission spectra of the $Sm^{3+}$-doped $SrWO_4:Sm^{3+}$ fluorescent powder. Figure 4c depicts the excitation spectrum of the $SrWO_4:Sm^{3+}$ fluorescent powder measured at room temperature and 650 nm. The excitation peak is caused by the *f–f* transition absorption of $Sm^{3+}$ ions and appears at 364, 377, 406, 445, and 481 nm, corresponding to $^6H_{5/2} \rightarrow {}^4D_{15/2}$, $^6H_{5/2} \rightarrow {}^4D_{1/2}$, $^6H_{5/2} \rightarrow {}^4K_{11/2}$, $^6H_{5/2} \rightarrow {}^4M_{19/2}$, and $^6H_{5/2} \rightarrow {}^4I_{13/2}$, respectively. Figure 4c displays excitation peaks at 406 and 481 nm, and Fig. 4d exhibits the emission spectrum of $SrWO_4:Sm^{3+}$ fluorescent powder under the excitation of near-UV light with a wavelength of 406 nm. Figure 4d indicates that the $SrWO_4:Sm^{3+}$ sample contains four emission peaks. The peak positions are 568, 602, and 650 nm, with an emission peak at 650 nm, which has the maximum luminescence intensity. The peak at 568 nm is attributed to the $^4G_{5/2} \rightarrow {}^6H_{5/2}$ transition in the 550–570 nm band, the peaks at 602 nm correspond to the $^4G_{5/2} \rightarrow {}^6H_{7/2}$ transition in the 575–630 band, and the peak at 650 nm corresponds to the $^4G_{5/2} \rightarrow {}^6H_{9/2}$ transition in the 630–650 nm band. These four emission peaks are caused via *f–f* transitions in the 4*f* electron shell of the $Sm^{3+}$ ion [15, 16]. As seen, the LED chip can excite the $Sm^{3+}$-doped $SrWO_4:Sm^{3+}$ fluorescent powder in the UV-visible light region. It is expected that matching the powder with yellow-green powder will achieve high-efficiency white LED luminescence.

Figures 4e,f depict the excitation and emission spectra of the rare earth $Pr^{3+}$-doped $SrWO_4:Pr^{3+}$ fluorescent powder. Figure 4e illustrates the excitation spectrum of the $SrWO_4:Pr^{3+}$ fluorescent powder at 657 nm. Figure 4e reveals that the excitation spectrum of $SrWO_4:Pr^{3+}$ fluorescent powders has three distinct $Pr^{3+}$ excitation peaks. The main excitation peaks are observed at 453, 477, and 490 nm and are respectively attributed to the energy level transitions of $^3H_4 \rightarrow {}^1I_6$, $^3H_4 \rightarrow {}^3P_1$, and $^3H_4 \rightarrow {}^3P_0$ of $Pr^{3+}$. This demonstrates that the $SrWO_4:Pr^{3+}$ fluorescent powder can be effectively excited by blue light with a wavelength range of 450–500 nm, enabling it to adequately match the emission of the blue LED chip. Figure 4f demonstrates the emission spectrum of the $Pr^{3+}$-doped $SrWO_4:Pr^{3+}$ fluorescent powder detected at 453 nm. Figure 4f illustrates that all of the emission spectra resulting from the 4*f*–4*f* characteristic transitions of $Pr^{3+}$ have an emission peak at 657 nm, which is attributed to the $^3P_0 \rightarrow {}^3F_2$ electric dipole transition of $Pr^{3+}$. The emission peaks at 610 nm and 626 nm are attributed to the $^1D_2 \rightarrow {}^3H_4$ and $^3P_0 \rightarrow {}^3H_6$ transitions, respectively. As seen, the blue LED can effectively excite the $SrWO_4:Pr^{3+}$ red fluorescent powder and generate red light [17].

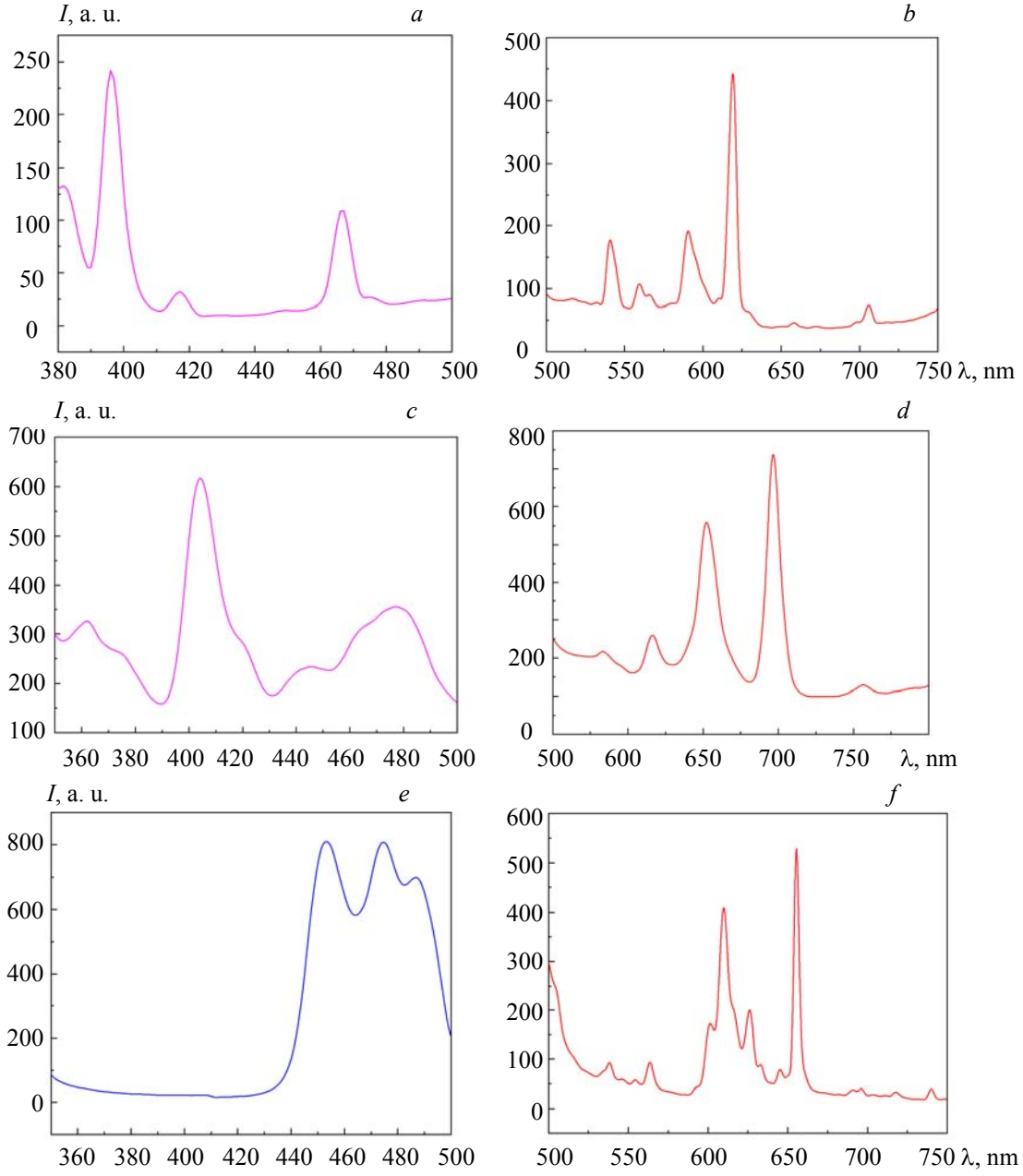


Fig. 4. Excitation (a, c, e) and emission (b, d, f) spectra of $SrWO_4:Eu^{3+}$ (a, b), $SrWO_4:Sm^{3+}$ (c, d), and $SrWO_4:Pr^{3+}$ (e, f) phosphors.

*Testing an LED device and determining CIE chromaticity coordinates.* In the $SrWO_4:RE^{3+}$(RE = Eu, Sm, Pr) fluorescent powder, the excitation peak of $SrWO_4:Eu^{3+}$ red powder is located at 395 nm, which is highly matched with the UV 395 nm chip in the market. Therefore, $SrWO_4:Eu^{3+}$ can be employed as the red powder in three primary colors with the commercial green powder $(Ba,Sr)_2SiO_4:Eu^{2+}$ and the commercial blue powder BAM. The approximate mass ratio of the three components is 8:1:2. A 310 nm deep UV chip is coated with ZWL8820 organic silica gel and dried at 110°C for 1 h to obtain a white LED device with a forward bias current of 60 mA. Figure 5 depicts the spectrum and chromaticity coordinates of the device. Furthermore, the color rendering indexes of the device are $R_a$ = 92.7 and CRI = 89.5; the color temperature is 6685 K, and the color coordinates are (0.3056, 0.3256), demonstrating that the LED device can successfully emit white light.

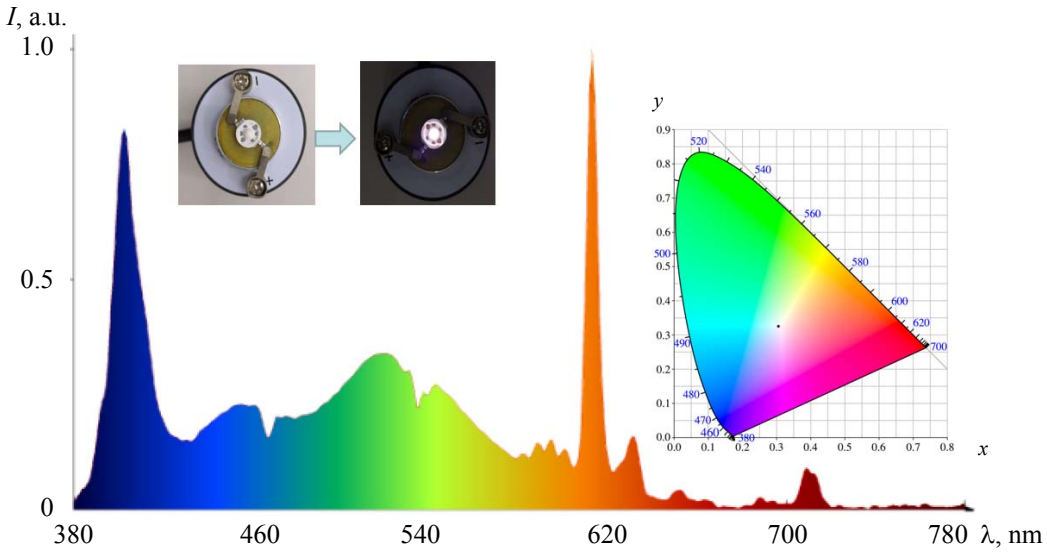


Fig. 5. Spectra of white LED prototypes and CIE chromaticity coordinates.

**Conclusions.** The high-temperature solid-phase method has been used to synthesize $SrWO_4:RE^{3+}$ (Re = Eu, Sm, Pr) fluorescent powders with a spherical-like morphology. The main excitation peaks of these fluorescent powders were observed at 395, 406, and 453 nm, indicating that this type of fluorescent powder is appropriate for excitation from the UV region to the visible light region. Meanwhile, the main red emission peaks are located at 616, 650, and 657 nm. A white LED device was constructed by combining $SrWO_4:Eu^{3+}$ red fluorescent powder with commercially available green and blue fluorescent powders. The chromaticity coordinates were (0.3055, 0.3532); the color rendering indexes were $R_a$ = 92.7 and CRI = 89.5, and the color temperature was 6685 K. $SrWO_4:RE^{3+}$ (RE = Eu, Sm, Pr) fluorescent powders are superior luminescent materials that can be excited by UV-Vis light and are expected to be red fluorescent powders for white LEDs.

**Acknowledgements.** This work was financially supported by Xi'an Science and Technology Committee Program (No. GXYD9.2) and Shan'xi Educational Committee of the National Natural Science (No. 17JK0395).

## REFERENCES

1. M. Song, W. Ran, Y. Ren, et al., *J. Alloys and Comp*., **865**, 158825 (2021).
2. Li Zhao, Wang Yongfeng, Cao Jing, J. Wuhan, *Materials Science, University of Technology*, **33**, No. 5, 1028 (2018).
3. Li Zhao, Wu Kunyao, Wang Yanan, et al., *Ferroelectrics*, **582**, No. 1, 63 (2021).
4. Ling Junrong, Zhou Youfu, Xu Wentao, et al., *J. Adv. Ceram*., **9**, No. 1, 45 (2020).
5. P. Phogat, S. P. Khatkar, R. K. Malik, et al., *J. Luminescence*, **234**, 117984 (2021).
6. H. Zhang, Y. Chen, X Zhu, et al., *J. Luminescence*, **236**, 118131 (2021).
7. Li Zhao, Wang Yongfeng, Cao Jing, et al., *J. Rare Earths*, **34**, No. 2, 143 (2016).
8. Li Zhao, Zhao Xicheng, Jiang Yuanru, et al., *J. Rare Earths*, **33**, No. 1, 33 (2015).
9. Peng Xiao, Yang Weiwei, Ling Dongxiong, et al., *Chin. J. Lumin*., **42**, No. 4, 7 (2021).
10. Jiang Hongxi, Lv Shuchen, *Acta Phys. Sinica*, **70**, No. 17, 278 (2021).
11. Li Zhao , Wu Kunyao , Wang Yongfeng, et al., *Chin. J. Mater. Res*., **31**, No. 4, 274 (2027).
12. Li Zhao, Wang Yongfeng, Cao Jing, et al., *Spectrosc. and Spectr. Analysis*, **40**, No. 10, 4 (2020).
13. L. Qin, J. Chen, X. Chen, et al., *J. Luminescence*, **238**, 118228 (2021).
14. G. E. Malashkevich, V. N. Sigaev, N. V. Golubev , et al., *JETP Lett*., **92**, No. 8, 497 (2010).
15. G. E. Malashkevich, I. M. Mel'nichenko, E. N. Poddenezhnyi, et al., *Phys. Solid State*, **40**, No. 3, 420 (1998).
16. M. N. Singh, L. R. Singh, A. G. Barua, *Rad. Phys. Chem*., **188**, 109631 (2021).
17. J. W. Chung, H. K. Yang, B. K. Moon, et al., *J. Nanosci. Nanotechnol*., **11**, No. 7, 6208 (2011).